Positive/Negative Refractive Index Anisotropic 2-D Metamaterials

Christophe Caloz and Tatsuo Itoh

***Abstract*—An anisotropic metamaterial, based on a transmission line (TL) approach, that exhibits positive refractive index (PRI) in one direction and negative refractive index (NRI) in another (orthogonal) direction is presented, characterized and demonstrated in terms of analytic dispersion diagrams, equivalent refractive indexes, and circuit-simulated voltage/current/power distributions. This anisotropic structure may also be implemented in distributed architectures and lead to novel antenna and reflector applications.**

I. Introduction

RECENTLY, there has been significant interest for metamaterials, and in particular for materials with simultaneously negative permittivity and permittivity, or left-handed (LH) materials, originating from a theoretical speculation of Veselago in 1968 [1]. Some milestones of this research include the negative permittivity thin-wires plasma structure [2], the negative permeability split-rings plasma structure[3], the experimental demonstration of a composite LH structure[4], the subwavelength superlens [5], and the introduction of an efficient transmission line (TL) approach of metamaterials[6], [7] with several practical microwave applications[8].

In this paper, we present a novel anisotropic TL 2-D metamaterial that exhibits positive refractive index (PRI) in one direction and negative refractive index (NRI) in another direction, and therefore supporting right-handed (RH) waves in the PRI-direction and LH waves in the NRI-direction. The structure consists of a 2-D periodic [9] array of inductors, capacitors and TL sections, and is analytically described by a 2-D TL model using transmission matrixes [10], and based on Kirchoff's laws and on the Bloch-Floquet theorem. Although the proposed structure is constituted of lumped-elements and TL sections, it may also be implemented in distributed (real physical metal/dielectric architectures) form with versatile characteristics [11].

II. PRI/NRI Anisotropy

The proposed anisotropic structure consists of the periodic repetition of the anisotropic TL unit cell depicted in Fig. 1(a) forming a 2-D array. It represents the combination of an isotropic RH and isotropic LH structures. In the xy-plane, the structure includes inductances of value $L_R/2$ and transmission line sections of length $a/2$ along the x-direction, while it includes capacitances of value $2C_L$ and transmission line sections of length $a/2$ along the y-direction. At low frequencies, propagation occurs mainly along the x-direction because the y-directed capacitors are open circuits, and the unit cell reduces to the RH model shown in Fig. 1(b). Thus, at low frequencies the structure exhibits a PRI and will support a RH wave along the x-direction. In contrast, at high frequencies, it is the x-directed inductors which become open circuits while the impedance of the y-directed capacitors decreases. As a consequence, propagation occurs mainly along the y-direction, and the unit cell reduces to the LH model shown in Fig. 1(c). Thus, at high frequencies the structure exhibits a NRI and will support a LH wave along the y-direction.

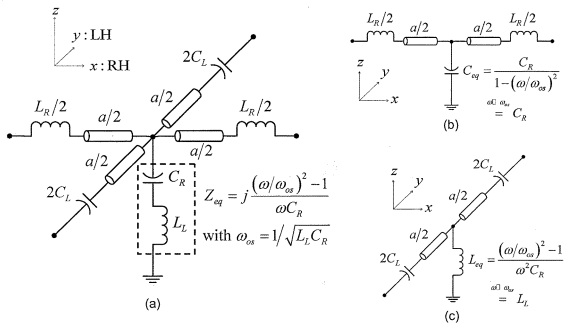

Fig. 1. Circuit model for the unit cell of the 2-D anisotropic structure. (a) Anisotropic structure with PRI (RH) along x and NRI (LH) along y. (b) Equivalent RH circuit at low frequencies. (c) Equivalent LH circuit at high frequencies.

In terms of constitutive parameters, the proposed structure may be represented by the anisotropic permittivity, permeability and refractive index tensors

$$[\varepsilon] = \begin{bmatrix} \varepsilon_x = C' + \frac{C_R}{a} & 0 \\ 0 & \varepsilon_y = C' - \frac{1}{(\omega^2 L_L a)} \end{bmatrix} \quad (1)$$

$$[\mu] = \begin{bmatrix} \mu_x = L' + \frac{L_R}{a} & 0 \\ 0 & \mu_y = L' - \frac{1}{(\omega^2 C_L a)} \end{bmatrix} \quad (2)$$

$$[n] = \begin{bmatrix} n_x = s_x\sqrt{\varepsilon_x \mu_x} & 0 \\ 0 & n_y = s_y\sqrt{\varepsilon_y \mu_y} \end{bmatrix},$$

$$\text{with } s_{x,y} = \frac{1}{2}\left[\operatorname{sgn}(\varepsilon_{x,y}) + \operatorname{sgn}(\mu_{x,y})\right] \quad (3)$$

where L'/C' represent the per-unit-length inductance/capacitance of the transmission line sections, L_R/C_R and L_L/C_L are the inductance/capacitance ([H/F]) of the inductors/capacitors along x and y, respectively. The L'/C' parameters of a TL of characteristic impedance Z_0 and effective permittivity ε_{eff} are given by $C' = \sqrt{\varepsilon}_{eff}/(c_o Z_0)$ and $L' = Z_0\sqrt{\varepsilon}_{eff}/c_o$, respectively, where c_0 is the velocity of light. Thus, the permittivity, permeability and refractive index tensors can be fully determined from the structural parameters.

Manuscript received May 7, 2003; revised October 23, 2003. This work is part of the MURI program "Scalable and Reconfigurable Electromagnetic Metamaterials and Devices" and was supported by the Department of Defense (N00014–01-1–0803) and monitored by the U.S. Office of Naval Research.

The authors are with the Department of Electrical Engineering, University of California at Los Angeles, Los Angeles, CA 90095 USA (e-mail: caloz@ee.ucla.edu).

Digital Object Identifier 10.1109/LMWC.2003.820641

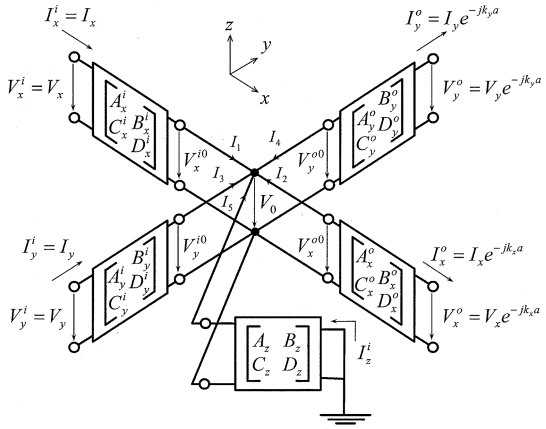

Fig. 2. Transmission line representation for the unit cell of a general 2-D metamaterial. Each branch is represented by the appropriate [*ABCD*] matrix. The Bloch-Floquet theorem was applied to relate the input (i) and output (o) currents and voltages assuming a unit-cell of length (or period) a.

III. Two-dimensional Transmission Line Analysis

A 2-D metamaterial may be represented by the transmission line unit cell shown in Fig. 2, where each branch of the circuit is represented by its [*ABCD*] or transmission matrix. Applying Kirchhoff's voltage and current laws at the center node in conjunction with the Bloch-Floquet theorem (period $= a$) yields the following set of linear equations (see (4) at the bottom of the page). After eliminating I_z^i, we obtain the homogeneous system (see 5(a)-5(c) at the bottom of the page). The system (5) admits a nontrivial solution if $\det(M) = 0$. Solving for the spectral parameters (k_x, k_y) continuously sweeping the edge of the irreducible Brillouin zone yields the frequency solutions or the dispersion diagram of the structure.

In the particular case of the anisotropic structure of Fig. 1(a), the [*ABCD*] matrixes of the five branches are

$$\begin{bmatrix} A_x^i & B_x^i \\ C_x^i & D_x^i \end{bmatrix} = \begin{bmatrix} c - \frac{\omega Y_0 L_R s}{2} & j\left(Z_0 s + \frac{\omega L_R c}{2}\right) \\ jY_0 s & c \end{bmatrix} \tag{6a}$$

$$\begin{bmatrix} A_y^i & B_y^i \\ C_y^i & D_y^i \end{bmatrix} = \begin{bmatrix} c + \frac{Y_0 s}{2\omega C_L} & j\left[Z_0 s - \frac{c}{2\omega C_L}\right] \\ jY_0 s & c \end{bmatrix} \tag{6b}$$

$$\begin{bmatrix} A_x^o & B_x^o \\ C_x^o & D_x^o \end{bmatrix} = \begin{bmatrix} c & j\left(\frac{\omega L_R c}{2} + Z_0 s\right) \\ jY_0 s & -\frac{\omega Y_0 L_R s}{2} \end{bmatrix} \tag{6c}$$

$$\begin{bmatrix} A_y^o & B_y^o \\ C_y^o & D_y^o \end{bmatrix} = \begin{bmatrix} c & j\left(Z_0 s - \frac{c}{2\omega C_L}\right) \\ jY_0 s & \frac{Y_0 s}{2\omega C_L} \end{bmatrix} \tag{6d}$$

$$\begin{bmatrix} A_z & B_z \\ C_z & D_z \end{bmatrix} = \begin{bmatrix} 1 & \frac{\left(1-\omega^2 C_R L_L\right)}{(j\omega C_R)} \\ 0 & 1 \end{bmatrix} \tag{6e}$$

where $c = \cos(ka/2)$, $s = \sin(ka/2)$ with $k = \omega/c_0$, and $Y_0 = 1/Z_0$.

$$\begin{cases} V_x^{i0} = V_0 = \frac{D_x^i V_x - B_x^i I_x}{A_x^i D_x^i - B_x^i C_x^i} \\ V_y^{i0} = V_0 = \frac{D_y^i V_y - B_y^i I_y}{A_y^i D_y^i - B_y^i C_y^i} \\ V_x^{o0} = V_0 = \left(A_x^0 V_x + B_x^0 I_x\right) e^{-jk_x a} \\ V_y^{o0} = V_0 = \left(A_y^o V_y + B_y^o I_y\right) e^{-jk_y a} \\ V_0 = -\frac{B_Z I_Z^i}{A_Z D_Z - B_Z C_Z} \\ \sum_{k=1}^{5} I_k^{\text{node}} = \frac{\left(-C_x^i V_x + A_x^i I_x\right)}{A_x^i D_x^i - B_x^i C_x^i} + \frac{\left(-C_y^i V_y + A_y^i I_y\right)}{A_y^i D_y^i - B_y^i C_y^i} - \left(C_x^o V_x + D_x^o I_x\right) e^{-jk_x a} \\ \qquad - \left(C_y^o V_y + D_y^o I_y\right) e^{-jk_y a} + \frac{A_z I_z^i}{A_z D_z - B_z C_z} = 0 \end{cases} \tag{4}$$

$$M = \begin{bmatrix} \alpha - \frac{A_z D_x^i}{B_z \Delta_x^i} & \beta + \frac{A_z B_x^i}{B_z \Delta_x^i} & \gamma & \delta \\ \alpha & \beta & \gamma - \frac{A_z D_y^i}{B_z \Delta_y^i} & \delta + \frac{A_z B_y^i}{B_z \Delta_y^i} \\ \alpha - \frac{A_x^0 A_z e_x}{B_z} & \beta - \frac{A_z B_x^o e_x}{B_z} & \gamma & \delta \\ \alpha & \beta & \gamma - \frac{A_y^o A_z e_y}{B_z} & \delta - \frac{A_z B_y^o e_y}{B_z} \end{bmatrix}$$

$$\times \begin{bmatrix} V_x \\ I_x \\ V_y \\ I_y \end{bmatrix} = \begin{bmatrix} 0 \\ 0 \\ 0 \\ 0 \end{bmatrix} \tag{5a}$$

$$\text{where } \alpha = -C_x^o e_x - \frac{C_x^i}{\Delta_x^i}, \beta = -D_x^o e_x + \frac{A_x^i}{\Delta_x^i},$$

$$\gamma = -C_y^o e_y - \frac{C_y^i}{\Delta_y^i}, \delta = -D_y^o e_y + \frac{A_y^i}{\Delta_y^i} \tag{5b}$$

$$\text{with } \Delta_k^i = A_k^i D_k^i - B_k^i C_k^i \ (k = x, y)$$

$$\text{and } e_x = e^{-jk_x a}, e_y = e^{-jk_y a} \tag{5c}$$

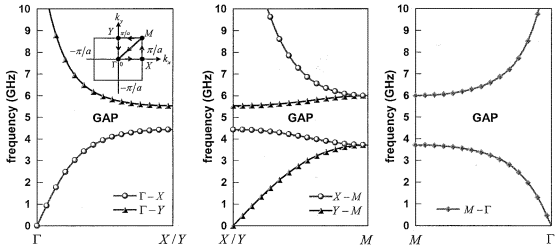

Fig. 3. Dispersion diagram for the structure Fig. 1(a) with the parameters $C_R = C_L = 1\,\mathrm{pF}$, $L_R = L_L = 1\,\mathrm{nH}$, a $= 1\,\mathrm{mm}$, $f_c^{\mathrm{LP-RH}} = 4.5\,\mathrm{GHz}$ and $f_c^{\mathrm{HP-LH}} = 4.5\,\mathrm{GHz}$.

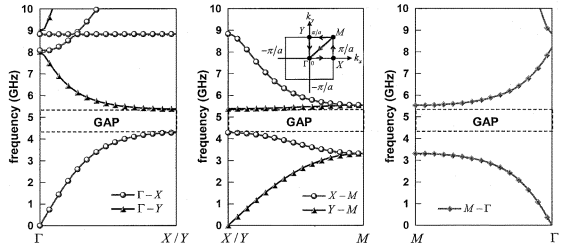

Fig. 4. Dispersion diagram for longer lengths for the same parameters as in Fig. 3, except $a = 3\,\mathrm{mm}$.

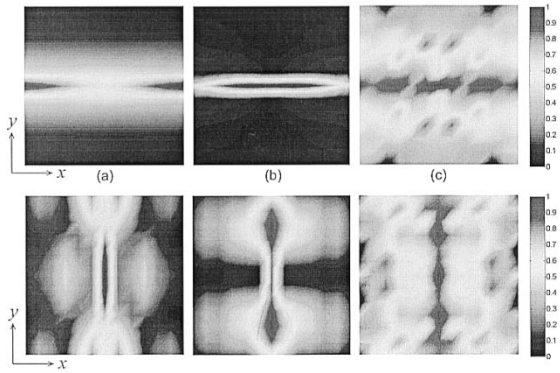

Fig. 5. Distributions in the 2-D anisotropic structure corresponding to Fig. 3 at $f = 2\,\mathrm{GHz}$ (RH range) and at $f = 2\,\mathrm{GHz}$(LH range). (a) $f = 2\,\mathrm{GHz}$ voltage magnitude. (b) $f = 2\,\mathrm{GHz}$ current magnitude (y-component). (c) $f = 2\,\mathrm{GHz}$ power. (d) $f = 5\,\mathrm{GHz}$ voltage magnitude. (e) $f = 5\,\mathrm{GHz}$ current magnitude (y-component). (f) $f = 5\,\mathrm{GHz}$ power.

IV. Dispersion Diagrams and Fields Distributions

Fig. 3 shows a typical dispersion diagram for the anisotropic structure of Fig. 1(a). The dispersion slopes are positive/negative along the $\Gamma - X/\Gamma - Y$ paths, which reveal the PRI/NRI of the structure along the x/y-directions, as expected from Fig. 1. At low frequencies, propagation occurs mainly along the x-direction with linear-RH (forward wave with phase lag) characteristics. As frequencies is increased, the cutoff-proximity effect of the low-pass structure of Fig. 1(b) asymptotically bends the curve to a horizontal line (zero group velocity), corresponding to the resonance $f_c^{\mathrm{LP-RH}} = 1/\pi\sqrt{L_R C_{eq}}$, which opens up a gap extending up to the cutoff frequency of the y-direction high-pass structure of Fig. 1(c), given by $f_c^{\mathrm{LP-RH}} = 1/4\pi\sqrt{L_R C_{eq}}$. Above $f_c^{\mathrm{LP-RH}}$, the -direction hyperbolic-LH (backward wave with phase advance) mode is excited.

In practical structures, the RH-TL interconnects shown in Fig. 1 are always present. To illustrate their effect, we consider the same structure as in Fig. 3, but with longer TL interconnects in Fig. 4. It can be seen that as the interconnects TL length a increases, the y-LH mode starts to depart from its ideal hyperbolic nature with $\omega(\beta \to 0) \to \infty$; here the fundamental y-LH mode crosses the $\beta = 0$ axis at 8 *GHz*, and a second y-mode (RH) emerges just above.

Note that the (frequency dispersive) refractive index associated with the different modes could be straightforwardly determined approximately from (3) or accurately from the dispersion diagram using the relation $n(f) = c_0\beta(f)/(2\pi f)$, $\beta(f)$ being the computed dispersion relation.

Fig. 5 shows voltage, current and power distributions in the anisotropic structure, obtained with the circuit simulator of the commercial software Ansoft-HFSS. The structure consists an array of 13×13 cells and is excited by a sinusoidal voltage source at the center. It appears clearly that propagation occurs predominantly along the x-direction at 2 GHz and along the y-direction at 8 GHz, as predicted from the dispersion diagram. This fact, in conjunction with the sign of the dispersion slopes, demonstrates the x-PRI/y-NRI anisotropy of the structure and validates the approximate models of Figs. 1(b) and 1(c).

V. Conclusion

A novel anisotropic 2-D TL structure exhibiting PRI along one direction at low frequencies and NRI along the other orthogonal direction at higher frequencies was introduced, characterized and demonstrated in terms of exact analytic dispersion diagrams and voltage/current/power distributions. In addition to demonstrating and characterizing PRI/NRI anisotropic metamaterials, the present contribution may lead to novel applications based on anisotropic structures using distributed textured surfaces for antennas and reflectors with distinct responses for orthogonal linear polarizations.

References

[1] V. G. Veselago, "The electrodynamics of substances with simultaneously negative values of ε and μ," *Soph. Phys. Usp.*, vol. 10, no. 4, pp. 509–514, Jan.-Feb. 1968.

[2] J. B. Pendry, A. J. Holden, W. J. Stewart, and I. Youngs, "Extremely low frequency plasmons in metallic mesostructures," *Phys. Rev. Lett.*, vol. 76, no. 25, pp. 4773–4135, June 1996.

[3] J. B. Pendry, A. J. Holden, and W. J. Stewart, "Magnetism from conductors and enhanced nonlinear phenomena," *IEEE Trans. Microwave Theory Tech.*, vol. 47, pp. 2075–2084, Nov. 1999.

[4] R. A. Schelby, D. R. Smith, and S. Schultz, "Experimental verification of negative index of refraction," *Science*, vol. 292, pp. 77–79, Apr. 2001.

[5] J. B. Pendry, "Negative refraction makes a perfect lens," *Phys. Rev. Lett,.*, vol. 85, no. 18, pp. 3966–3969, Oct. 2000.

[6] C. Caloz, H. Okabe, T. Iwai, and T. Itoh, "Transmission line approach of left-handed (LH) materials," in *USNC/URSI National Radio Science Meeting*, vol. 1, San Antonio, TX, June 2002, p. 39.

[7] G. V. Eleftheriades, A. K. Iyer, and P. C. Kremer, "Planar negative refractive index media using periodically *L-C* loaded transmission lines," *IEEE Trans. Microwave Theory Tech.*, vol. 50, pp. 2702–2712, Dec. 2002.

[8] C. Caloz and T. Itoh, *IEEE-MTT Int. Symp. Focused Session.*, vol. 1, Philadelphia, PA, June 2003, pp. 195–198.

[9] L. Brillouin, *Wave Propagation in Periodic Structures*, 2nd ed. New York: Dover, 1946.

[10] D. M. Pozar, *Microwave Engineering*, 2nd ed. New York: Wiley, 1998.

[11] A. Sanada, C. Caloz, and T. Itoh, "2D distributed periodic structures with anisotropic LH and RH characteristics," in *Progress in Electromagnetics Research Symp. (PIERS)*, Waikiki, HI, Oct. 2003.